

Optimization of Fuel Consumption with Respect to Orbital Requirements for High Resolution Remote Sensing Satellite Constellations

**Drago Matko, Tomaž Rodič, Krištof Oštir, Aleš Marsetič, Marko Peljhan, Sašo Blažič, Gregor Klančar,
Gašper Mušič**
Space-SI

Aškerčeva cesta 12, 1000 Ljubljana, Slovenia; Tel. +386 1 4768252
drago.matko@space.si

ABSTRACT

Among applications of formation flying, several case scenarios for High Resolution Remote Sensing Satellite Constellations were proposed in the literature. For a radar interferometric system a pair of satellites has to be at two different positions that are separated by a distance of several hundred meters during measurement sequence. The satellites can be either in the same orbit or in a part of approximately parallel orbits. During imaging the relative separation of the satellites has to be stable and precisely known. In the case of an optical payload, one satellite can hold the optical lens system and the other the imaging sensors. The satellites must fly one over the other or one behind the other at a close range. In the paper, several manoeuvres for Satellite Constellations are analysed and simulated with the respect to fuel consumption. A linear model based on Hill-Clohessy-Wiltshire equations is solved analytically for the fuel consumption analysis. Linear models are optimised serving an approximate solution with respect to optimal fuel consumption respecting constraints, such as maximal disposable time and the instant of required formation position. Better results are obtained when orbit eccentricity is taken into account, as shown in the simulated examples.

INTRODUCTION

In Slovenia a new Centre of Excellence for Space Sciences and Technologies SPACE-SI has been established in 2010 with the main focus on nano and micro satellite technologies. The Research & Technical Development (RTD) goals of the SPACE-SI consortium consisting of academic institutions, high-tech SMEs and large industrial and insurance companies are focused on nano and micro satellite technologies that are enabling high precision interactive remote sensing and precise maneuvering of small spacecrafts in formation flying missions. For the development of these technologies an advanced RTD infrastructure will be set up including a multidisciplinary laboratory for closed-loop investigations of materials, structures, micropropulsion systems, electronic components and visual based control algorithms in simulated space environments. The experimental techniques will be combined with virtual models for primal and sensitivity analyses of components, subsystems and platforms as well as for their characterisation by inverse numerical analyses and optimisation of their design with respect to performance and reliability. The development of a technology demonstration mission is envisaged for which synergies and potential partners are sought at the international level.

Nano satellites such as the Cubesat family, for example, are also very popular and affordable means for training young scientists and engineers at universities with ambitious multidisciplinary goals in space RTD. Introduction of Commercial off-the-shelf (COTS) components has reduced the costs of small satellites to such a level that failure of a satellite system is no longer considered as catastrophe but rather as a manageable risk. This allows introduction of new creative paradigms permitting high risk – high benefit approaches in space system design and mission planning which are expected to accelerate technology development in unprecedented ways. The indicated transitions have opened opportunities for newcomers to the space arena, including RTD players from economically less powerful and aerospace developed regions. In a similar way one could define RTD challenges for other types of missions which offer great Science and technology (S&T) opportunities for the small satellite sector. This opens very large RTD areas where we have identified the most promising RTD targets with an additional added value, that will be achieved by harmonising individual RTD strategies of laboratories by focussing on a common multidisciplinary goal targeted on enabling technologies for advanced platform manoeuvring.

In recent years there has been an increased interest in formation flying satellites and autonomous docking.

The formation flying satellites offer potentially greater science and operational capabilities than those attainable with a monolithic spacecraft. Not only the modules from a large and expensive monolithic satellite are distributed to a number of smaller and cheaper platforms, but even more importantly a whole spectrum of new missions (such as stereo vision) that could be performed by a group of satellites is made possible.

Fundamentals of astrodynamics and a comprehensive treatment of dynamics of space systems including formation flying is provided in [1,2]. Simulation of spacecraft attitude and orbit dynamics with quaternions is given in [3]. Similar simulation in object-oriented program Modelica is presented in [4]. Dynamics of earth orbiting formations and linear models of formations based on Hill-Clohessy-Wiltshire (HCW) equations are given in [5,6], while geometry and control of satellite formations are described in [7]. Linear and non-linear models are also given in [8], where also impulse and continuous control, disturbances, period matching controllers and formation configurations are discussed. Architecture for spacecraft formation control is discussed in [9]. Satellite relative motion propagation and control in the presence of J_2 perturbations is given in [10]; analysis of the perturbed J_2 for spacecraft formation flight and modified HCW equations are presented in [11] and relative orbital configurations in [12]. Development of guidance, navigation and control architecture and validation process enabling autonomous docking to a tumbling satellite is presented in [13]. Impulsive feedback control and corresponding manoeuvres are discussed in [14]. A geometrical method for the path prediction based on the state transition matrix and its comparison with HCW equations are given in [15]. Closed-loop control of spacecraft formations with an application is demonstrated in [16] while the results of autonomous docking experiments in the presence of anomalies are given in [17]. Adaptive control of satellite formation flying and global output feedback tracking control of spacecraft formation flying with parametric uncertainty are presented in [18] and [19] respectively. Fault detection and diagnosis for a multiple satellite formation flying system is given in [20]. Formation flying with global positioning system (GPS) is discussed in [21]. Control and autonomy algorithms for docking are presented in [22]. Dynamics and control of spacecraft formations in the presence of disturbances is given in [23]. An intelligent control concept for formation flying satellites with aim to optimize fuel consumption is presented in [24]. Vision-based navigation for formation flying is given in [25,26]

In order to achieve the high autonomy and cooperation between the satellites, algorithms for autonomous

docking and formation flying (Guidance, Navigation and Control – GN&C algorithms) have to be developed and tested. These algorithms will, in combination with on-line path planning and obstacle avoidance algorithms ensure safe autonomous docking and will enable the desired formation of the satellites for a specific task.

Various scenarios using formation flying were presented in the literature, such as high-resolution dual satellite optical remote sensing, radar interferometric imaging and space debris observation

High-resolution optical dual satellite imaging is also called fractionated spacecraft. Close formation flying of small satellites enables several opportunities for high resolution remote sensing, so it is expected that High Resolution Remote Sensing Satellite Constellations (HRRSSC) will become an attractive solution for Earth observation. In the case of an optical payload, one satellite can hold the optical lens system and the other the imaging sensors. The satellites must fly one over the other or one behind the other if a mirror at an angle of approximately 45° is used to reflect the beam to the sensors. To obtain a multispectral resolution in the order of few meters, both satellites should be placed close one to the other. When imaging both systems have to be precisely aligned and kept at a constant relative distance and orientation. The distance between the optical system and sensors has to be known in micrometer scale.

For the radar interferometric system a pair of satellites has to be in two different orbits that are separated by a distance of several hundred meters (e.g. 100-200 m) during measurement sequence. The satellites can be either in the same orbit (along track) or in a part of approximately parallel orbits (across track). During imaging the relative separation of the satellites has to be stable and precisely known (in the range of millimeters) to enable interferometric processing and achieve good results. Synthetic Aperture Radar interferometry (InSAR) technique is an effective tool of topographic mapping and generation of global Digital Elevation Model (DEM) [28]. It utilizes phase information included in two SAR images obtained from two antennas. SAR systems can provide images in daylight or at night and in nearly all weather conditions. The DEM obtained with InSAR has fine spatial resolution and target elevation precision [29], [30]. Especially the application of monitoring natural hazards place very complicated requirements on DEM. It is believed that better knowledge of relative orbits may significantly contribute to the baseline estimation methods.

Space debris is the collection of objects in space that were used by previous missions and no longer serve any useful purpose. It is believed that this issue will become a serious problem in near future, as the orbits of these objects often overlap with trajectories of operational spacecraft, and represent a potential collision risk. In order to remove the debris, close observation is necessary where during one or several encirclings the debris may be modelled as a 3D object. In order to have diversified images, the relative orbit planes must be as different as possible.

In this paper close formation will be discussed, i.e. the satellites will be considered to fly at distance less than a few hundred meters. In spacecraft formation flying mission design, the relative spacecraft position is more important than the knowledge of the absolute position of the formation [27]. In addition, knowledge of the relative states of spacecraft in a formation is often far more accurate than knowledge of the formation's absolute state. For these reasons, this paper will be focused on studies of the relative positions of two spacecraft, forming the formation. The satellites will be called leader and follower. Leader is supposed to be in the centre of the local vertical/local horizontal (LVLH), sometimes also called Radial/In-track/Cross-track (RIC), coordinate system. Its coordinates will be (0,0,0) all the times and its absolute position (orbit) will not be controlled. The leader may also be called target satellite since in some scenarios; it will represent the target to be observed or approached. Several manoeuvres will be analysed and simulated with the respect to fuel consumption. As fuel consumption is one of major constraints during a mission, linear mathematical models for formation flying will be developed next in an analytical form which enables fuel consumption estimation. In the next sections the derived models will be applied to different manoeuvres. The linear models are valid only for circular orbits without disturbances. An extension of linear models to orbits with small eccentricity is presented next. The paper concludes the presentation of simulation results.

MANOEUVRES

Formation flying can be performed by different manoeuvres which will be described in this section

Parallel flying – In-track displacement. This formation, where both satellites fly in a constant In-track displacement, is also called Along track flying or Trailing formation. It is applicable to high-resolution optical dual satellite imaging (fractionated spacecraft), where the displacement is in the range of a few meters, and Radar interferometry, where the displacement is in the range of a few hundred meters. The problem with this constellation is to keep both satellites in a constant

displacement and as shown later; this problem arises due to orbit eccentricity and disturbances.

Parallel flying – Radial displacement. This formation, where both satellites fly in a constant Radial displacement, is applicable to high-resolution optical dual satellite imaging (fractionated spacecraft). It is also called Nadir observation constellation. The displacement is in the range of a few meters. The problem with this constellation is to keep both satellites in a constant displacement and as shown later; this constellation can be held only with constant propulsion.

Parallel flying – Cross-track displacement. This formation, where both satellites fly in a constant Cross-track displacement, is applicable in Radar interferometry, where the displacement is in the range of a few hundred meters. The problem with this constellation is to keep both satellites in a constant displacement and as shown later; this constellation can be held only with constant propulsion.

Circumvolution of the target in the x-y plane. In this manoeuvre the follower flies around the target. This constellation is applicable to Space debris observation. As shown later, the circumvolution in the Radial-in-track plane is on an ellipse; by adding a Cross-track movement, a circular motion can be obtained where the follower is **encircling** the target.

Changing the In-track displacement. This manoeuvre is needed in order to change the formation. As shown later, the required fuel consumption is inverse proportional to the time needed for formation change.

Changing the Radial displacement. This manoeuvre is needed in order to change the formation. As shown later, it can be done in two ways with different fuel consumption results. However it can-not be done as a pure single transition; the change of the radial position is inevitably accompanied by a change in the In-track displacement. The way of performing the scenario depends on the sequence of manoeuvres. One of possible sequence of manoeuvres is the transition to the nadir observation constellation

Changing the Cross-track displacement. This manoeuvre is needed in order to change the formation. As shown later, the Cross-track motion is practically decoupled from the Radial and In-track motions.

FORMATION FLYING MODELS

The most common way to describe formation flying are the nonlinear Hill-Clohessy-Wiltshire (HCW) equations:

$$\begin{aligned}\ddot{x} - 2\dot{\phi}_R \dot{y} - \ddot{\phi}_R y - \dot{\phi}_R^2 x &= -\frac{\mu(R+x)}{((R+x)^2 + y^2 + z^2)^{\frac{3}{2}}} + \frac{\mu}{R^2} \\ \ddot{y} + 2\dot{\phi}_R \dot{x} + \ddot{\phi}_R x - \dot{\phi}_R^2 y &= -\frac{\mu y}{((R+x)^2 + y^2 + z^2)^{\frac{3}{2}}} \\ \ddot{z} &= -\frac{\mu z}{((R+x)^2 + y^2 + z^2)^{\frac{3}{2}}}\end{aligned}\quad (1)$$

where x , y and z are the coordinates of the target satellite in the local vertical/local horizontal (LVLH), sometimes also called Radial/In-track/Cross-track (RIC), coordinate system and the movement of the first satellite is described by:

$$\ddot{R} = R\dot{\phi}_R^2 - \frac{\mu}{R^2} \quad (2)$$

$$\ddot{\phi}_R = -\frac{2\dot{R}\dot{\phi}_R}{R} \quad (3)$$

These equations include the influence of the eccentricity and nonlinear differential gravitations. For close formation flying and small eccentricities these equations can be linearized with respect to x , y , z [8]

$$\begin{aligned}\ddot{x} - 2\dot{\phi}_R \dot{y} - \ddot{\phi}_R y - \dot{\phi}_R^2 x &= \frac{2\mu}{R^3} \\ \ddot{y} + 2\dot{\phi}_R \dot{x} + \ddot{\phi}_R x - \dot{\phi}_R^2 y &= -\frac{\mu}{R^3} y \\ \ddot{z} &= -\frac{2\mu}{R^3} z\end{aligned}\quad (4)$$

If the first satellite has a circular orbit ($R=a$), its angular acceleration is zero ($\ddot{\phi}_R = 0$), then its mean motion can be expressed by

$$\dot{\phi}_R = n = \sqrt{\frac{\mu}{a^3}} \quad (5)$$

Eqns. (1) are an equation for accelerations. If the satellite is accelerated by propulsion in x , y and z directions with accelerations a_x , a_y , and a_z , respectively, the linear HCW equations, describing the movement of the target satellite with the respect to the main one, are obtained as the following linear system of equations:

$$\begin{aligned}\ddot{x} - 2n\dot{y} - 3n^2 x &= a_x \\ \ddot{y} + 2n\dot{x} &= a_y \\ \ddot{z} + n^2 z &= a_z.\end{aligned}\quad (6)$$

For constant accelerations a_x , a_y , and a_z , this system of equations can be transformed into a homogenous one, using the following transformation

$$x = x_1 - \frac{1}{3n^2} a_x + 2a_y(t-t_0) \quad (7)$$

$$y = y_1 - \frac{3n}{2} a_y(t-t_0)^2 \quad (8)$$

$$z = z_1 + \frac{1}{n^2} a_z \quad (9)$$

Using these transformations Eqns.(6) can be transformed into

$$\begin{aligned}\ddot{x}_1 - 2n(\dot{y}_1 - 3na_y(t-t_0)) - \\ -3n^2(x_1 - \frac{1}{3n^2} a_x + 2a_y(t-t_0)) - a_x &= \\ = \ddot{x}_1 - 2n\dot{y}_1 - 3n^2 x_1 &= 0\end{aligned}\quad (10)$$

$$\begin{aligned}\ddot{y}_1 - 3na_y + 2n(\dot{x}_1 + 2a_y) - a_y = \\ = \ddot{y}_1 + 2n\dot{x}_1 &= 0\end{aligned}\quad (11)$$

$$\begin{aligned}\ddot{z}_1 + n^2(z_1 + \frac{1}{n^2} a_z) - a_z = \\ = \ddot{z}_1 + n^2 z_1 &= 0\end{aligned}\quad (12)$$

Linear equations (10), (11), (12) have with respect to initial conditions $x_1(t_0)$, $\dot{x}_1(t_0)$, $y_1(t_0)$, $\dot{y}_1(t_0)$, $z_1(t_0)$, $\dot{z}_1(t_0)$ the following solution

$$\begin{aligned}x_1(t) &= x_1(t_0)(4 - 3\cos nt) + \frac{\dot{x}_1(t_0)}{n} \sin nt + \frac{2\dot{y}_1(t_0)}{n}(1 - \cos nt) \\ y_1(t) &= y_1(t_0) + \dot{y}_1(t_0) \left[\frac{4}{n} \sin n(t-t_0) - 3(t-t_0) \right] + \\ &+ 6x_1(t_0) [\sin n(t-t_0) - n(t-t_0)] + \frac{2\dot{x}_1(t_0)}{n} \cdot (\cos n(t-t_0) - 1) \\ z_1(t) &= z_1(t_0) \cos n(t-t_0) + \frac{\dot{z}_1(t_0)}{n} \sin n(t-t_0)\end{aligned}\quad (13)$$

The solution of the non-homogenous system of equations(6) is then

$$\begin{aligned}
x(t) &= \left[x(t_0) + \frac{1}{3n^2} a_x \right] (4 - 3 \cos nt) + \frac{[\dot{x}(t_0) - 2a_y]}{n} \sin nt + \\
&+ \frac{2\dot{y}(t_0)}{n} (1 - \cos nt) + \frac{1}{3n^2} a_x + 2a_y (t - t_0) \\
y(t) &= y(t_0) + \dot{y}(t_0) \left[\frac{4}{n} \sin n(t - t_0) - 3(t - t_0) \right] + \\
&+ 6 \left[x(t_0) + \frac{1}{3n^2} a_x \right] \left[\sin n(t - t_0) - n(t - t_0) \right] + \\
&+ \frac{2[\dot{x}(t_0) - 2a_y]}{n} \cdot (\cos n(t - t_0) - 1) - \frac{3n}{2} a_y (t - t_0)^2 \\
z(t) &= \left[z(t_0) - \frac{1}{n^2} a_z \right] \cos n(t - t_0) + \frac{\dot{z}(t_0)}{n} \sin n(t - t_0) + \frac{1}{n^2} a_z
\end{aligned} \tag{14}$$

In the sequel the influence of initial condition on a non-propelled flight will be investigated.

THE INFLUENCE OF INITIAL CONDITIONS ON THE RELATIVE ORBIT

In this section the accelerations and all initial conditions but one will be set to zero, so the influence of a particular initial condition will be studied with respect to its application in different manoeuvres.

Influence of $x(t_0)$ – Initial Radial displacement

Linear equations (13) for $a_x = a_y = a_z = 0$ become:

$$\begin{aligned}
x(t) &= x(t_0)(4 - 3 \cos n(t - t_0)) \\
y(t) &= 6x(t_0) [\sin n(t - t_0) - n(t - t_0)] \\
z(t) &= 0
\end{aligned} \tag{15}$$

For short time

$$\begin{aligned}
\sin n(t - t_0) - n(t - t_0) &\approx 0 \\
\cos n(t - t_0) &\approx 1
\end{aligned}$$

so the satellites remain in constant relative position. Later the follower starts on oscillatory (amplitude $3x(t_0)$ in the x and $6x(t_0)$ in the y direction) drift of $12\pi x(t_0)$ meters per period in the negative direction of y .

This is because of the follower being on a higher – slower orbit.

By a constant acceleration $a_x = 3n^2 x(t_0)$ the satellites can be held in the initial constellation.

Influence of $y(t_0)$ – in track displacement

Linear equations (14) become:

$$\begin{aligned}
x(t) &= 0 \\
y(t) &= y(t_0) \\
z(t) &= 0
\end{aligned} \tag{16}$$

The follower follows the leader on the same orbit in the distance of initial displacement.

Influence of $\dot{x}(t_0)$ – Initial velocity in the radial direction

Linear equations (14) become:

$$\begin{aligned}
x(t) &= \frac{\dot{x}(t_0)}{n} \sin n(t - t_0) \\
y(t) &= \frac{2\dot{x}(t_0)}{n} (\cos n(t - t_0) - 1)
\end{aligned} \tag{17}$$

The relative orbit is an ellipse with the centre point of $-2\dot{x}(t_0)/n$. The y (In-track) semi axis of magnitude $2\dot{x}(t_0)/n$ is the major semi axis and is twice the length of the minor (Radial) semi axis. The ellipse is tangential to the x (Radial) axis at the starting point.

Influence of $\dot{y}(t_0)$ – Initial velocity in the In-Track direction

Linear equations (14) become:

$$\begin{aligned}
x(t) &= \frac{2}{n} \dot{y}(t_0) (1 - \cos n(t - t_0)) \\
y(t) &= \dot{y}(t_0) \left(\frac{4}{n} \sin n(t - t_0) - 3(t - t_0) \right) \\
z(t) &= 0
\end{aligned} \tag{18}$$

The relative movement at the satellites is a combination of an elliptical and linear (drifting) motion. The ellipse has the major semi axis of magnitude $4\dot{y}(t_0)/n$ in the y (in-track) direction and the minor semi-axis (half the major semi-axis) in the x (Radial) direction. It is tangential to the y (in-track) axis. The linear (drifting) motion is in the negative direction of the velocity which is three times the initial velocity. This results in the follower having to reduce speed in order to catch the leader, which is counter intuitive. The reason for this is that with the reduced velocity the follower transitions to a lower-faster orbit!

Influence of $z(t_0)$:

Linear equations (14) become

$$\begin{aligned} x(t) &= y(t) = 0 \\ z(t) &= z(t_0) \cos n(t-t_0) \end{aligned} \quad (19)$$

The z (Cross-track) motion is an oscillatory sinusoidal motion with the amplitude $z(t_0)$.

Influence of $\dot{z}(t_0)$

Linear equations (14) become

$$\begin{aligned} x(t) &= y(t) = 0 \\ z(t) &= \frac{\dot{z}(t_0)}{n} \sin n(t-t_0) \end{aligned} \quad (20)$$

The z - Cross-track motion is an oscillatory sinusoidal motion with the amplitude $\dot{z}(t_0)/n$.

Combined initial conditions

Since the model is linear, the combined initial conditions result in a linear combination of movements.

APPLICATION OF THE LINEAR MODEL TO DIFFERENT MANOEUVRES

Along track flying – trailing formation

With this scenario both satellites fly in constant In-track displacement D . The required initial conditions for this scenario are:

$$x(t_0) = 0, \quad y(t_0) = D, \quad \dot{x}(t_0) = 0, \quad \dot{y}(t_0) = 0 \quad (21)$$

With the linear model this constellation remains unchanged.

$$\begin{aligned} x(t) &= 0 \\ y(t) &= D \end{aligned} \quad (22)$$

The required fuel consumption is 0.

Changing the In-track displacement y

This scenario foresees the transition of the follower between two points along the orbit. The starting and final points are

$$\begin{bmatrix} x(t_0) \\ y(t_0) \\ z(t_0) \end{bmatrix} = \begin{bmatrix} 0 \\ 0 \\ 0 \end{bmatrix}, \quad \begin{bmatrix} x(t_f) \\ y(t_f) \\ z(t_f) \end{bmatrix} = \begin{bmatrix} 0 \\ Y \\ 0 \end{bmatrix} \quad (23)$$

As in the previous, also this manoeuvre will be in the x - y plane; the z component will remain 0. From the linear model it is obvious that the manoeuvre which satisfies the requirements is the application of $\dot{y}(t_0)$. With the manoeuvre duration equal to a multiple of the period

$$t_f = t_0 + N \frac{2\pi}{n}, \quad N = 1, 2, 3, \dots \quad (24)$$

equations (18) become

$$\begin{aligned} x(t_f) &= \frac{2}{n} \dot{y}(t_0) (1 - \cos 2N\pi) = 0 \\ y(t_f) &= \dot{y}(t_0) \left(\frac{4}{n} \sin 2N\pi - \frac{6N\pi}{n} \right) = -\frac{6N\pi}{n} \dot{y}(t_0) = Y \end{aligned} \quad (25)$$

yielding

$$\dot{y}(t_0) = -\frac{nY}{6N\pi} = -\frac{Y}{3TN} \quad (26)$$

When the transition is finished, the relative velocities in the x (Radial) and y (In-track) directions are

$$\begin{aligned} \dot{x}(t_f) &= \frac{nY}{3i\pi} \sin 2i\pi = 0 \\ \dot{y}(t_f) &= \frac{nY}{6i\pi} (4 \cos 2N\pi - 3) = \frac{nY}{6N\pi} \end{aligned} \quad (27)$$

To bring the follower to a stop his velocity must be 0, meaning that the same velocity change as in the beginning of the manoeuvre must be applied at its end in the opposite direction. This means that the total fuel consumption to mane the satellite along track is

$$FC = \frac{2Y}{3TN} \quad N = 1, 2, 3. \quad (28)$$

It can be seen that the fuel consumption can be arbitrarily reduced by prolonging the transition time. With the proposed scenario the transition time can be chosen arbitrarily but it must be a multiple of the orbit period. It must be pointed out that the proposed transition is a minimal fuel consumption transition. There are of course also other transitions possible, however with considerable higher fuel consumption.

Changing the x (Radial) position

This manoeuvre changes the height of an orbit by radial displacement x , starting at origin and will also remain entirely in the x - y plane. The starting and final points are

$$\begin{bmatrix} x(t_0) \\ y(t_0) \\ z(t_0) \end{bmatrix} = \begin{bmatrix} 0 \\ 0 \\ 0 \end{bmatrix}, \begin{bmatrix} x(t_f) \\ y(t_f) \\ z(t_f) \end{bmatrix} = \begin{bmatrix} X \\ 0 \\ 0 \end{bmatrix} \quad (29)$$

According to the linear model (Eqs. 14) there are two possibilities to do such a manoeuvre. With both possibilities the manoeuvre will be divided into two parts.

1. Applying the initial velocity in the x (Radial) direction

Eqs. (17) become

$$\begin{aligned} x(t_{f1}) &= \frac{\dot{x}(t_0)}{n} \sin n(t_{f1} - t_0) = X \\ y(t_{f1}) &= \frac{2\dot{x}(0)}{n} (\cos n(t_{f1} - t_0) - 1) \end{aligned} \quad (30)$$

Choosing the final time for the first transition of the manoeuvre

$$t_{f1} = t_0 + \frac{T}{4} \quad (31)$$

$x(t_{f1})$ becomes

$$x(t_{f1}) = \frac{\dot{x}(t_0)}{n} = X \Rightarrow \dot{x}(t_0) = nX \quad (32)$$

This equation determines the required initial velocity in the Radial direction. In track displacement $y(t_{f1})$ is then

$$y(t_{f1}) = -\frac{2\dot{x}(t_0)}{n} = -2X \quad (33)$$

which means that the change in the x (Radial) direction also results in the change in the y (In-track) displacement, which has to be compensated as shown next.

First the satellite has to be stopped at this intermediate position (0 in the radial direction and $-2X$ in the In-track direction). The velocity in this point due to the preceding transition is

$$\begin{aligned} \dot{x}(t_{f1}) &= X \cdot n \cdot \cos \frac{\pi}{2} = nX \\ \dot{y}(t_{f1}) &= -2 \sin \frac{\pi}{2} = 0 \end{aligned} \quad (34)$$

and has to be compensated what means that the same impulse (magnitude and direction) as at the start of the manoeuvre has to be applied.

To compensate, the In-track displacement for the manoeuvre described earlier, has to be applied for $Y = y(t_f)$. The initial velocity in the In-track direction must be

$$\dot{y} = -\frac{Y}{3TN} = \frac{n}{3\pi N} X \quad (35)$$

After N periods the same velocity change has to be applied in the opposite direction. The total fuel consumption (TFC) is then

$$\begin{aligned} TFC &= nX + \sqrt{(nX)^2 + \left(\frac{n}{3\pi N} X\right)^2} + \frac{n}{3\pi N} X = \\ &= nX \left(1 + \frac{1}{3\pi N} + \sqrt{1 + \frac{1}{(3\pi N)^2}}\right) \end{aligned} \quad (36)$$

Choosing one period ($N = 1$) for the second part of the manoeuvre, the fastest transition from the starting point to the end point given in Eq. (29) lasts 1.25 periods and consumes 2.1578 nX of fuel.

2. Applying the initial velocity in the y (In-track) direction

Eqs. (18) become

$$\begin{aligned} x(t_{f1}) &= \frac{2}{n} \dot{y}(t_0) (1 - \cos n(t_f - t_0)) = X \\ y(t_{f1}) &= \dot{y}(t_0) \left(\frac{4}{n} \sin n(t_f - t_0) - 3(t - t_0)\right) \end{aligned} \quad (37)$$

Choosing the final time for the first transition of the manoeuvre

$$t_{f1} = t_0 + \frac{T}{2} \quad (38)$$

$x(t_{f1})$ becomes

$$x(t_{f1}) = X = \frac{4}{n} \dot{y}(t_0) \Rightarrow \dot{y}(t_0) = \frac{n}{4} X \quad (39)$$

This equation determines the required initial velocity in the Radial direction. In-track displacement $y(t_{f1})$ is then

$$y(t_{f1}) = \frac{-3T}{2} \dot{y}(t_0) = \frac{-3\pi}{4} X \quad (40)$$

Again the change in the x (Radial) displacement causes the change in the y (In-track) displacement, which has to be compensated. First the satellite has to be stopped at the intermediate position ($x_{f1} = 0, y_{f1} = \frac{-3\pi}{4} X$). The velocity at this point is

$$\begin{aligned}\dot{x}(t_{f1}) &= \frac{2}{n} \left(\frac{n}{4} X\right) \cdot n \cdot \sin\left(\frac{2\pi}{T} \cdot \frac{T}{2}\right) = 0 \\ \dot{y}(t_{f1}) &= \frac{n}{4} X (4 \cos \pi - 3) = -\frac{7n}{4} X\end{aligned}\quad (41)$$

and has to be compensated. However in the same moment the next manoeuvre for compensating the In-track displacement of $Y = \frac{-3\pi}{4} X$ has to be initiated by changing the velocity in the same (y) direction.

For this the velocity change of

$$-\frac{Y}{3TN} = \frac{\pi}{4TN} X = \frac{n}{8N} X \quad (42)$$

has to be applied. The total velocity change at the intermediate point is then

$$\Delta\dot{y}(t_{f1}) = -\frac{7n}{4} x + \frac{n}{8N} x = \left(\frac{1}{8N} - \frac{7}{4}\right)nX \quad (43)$$

After N periods the velocity change $nX/(8N)$ has to be applied in the opposite direction.

The total fuel consumption is then

$$TFC = \frac{n}{4} X + \left| \frac{1}{8N} - \frac{7}{4} \right| nX + \frac{1}{8N} = 2nX \quad (44)$$

and is independent of N , which means that one period (fastest transition) chosen for the second part of the manoeuvre without any loss of fuel. It is obvious that this second manoeuvre consumes less fuel than the first one, but is a bit slower (1.5 period instead of 1.25).

Transition to the nadir observation constellation

Nadir constellation is defined by the endpoint $x(t_f) = x, y(t_f) = 0$. This constellation is suitable to continuously observe the nadir point. According to the results of the previous point there are again two possibilities to achieve this translation.

According to the first manoeuvre the starting point and applied velocity changes must be

$$\begin{aligned}x(t_0) &= 0 & y(t_0) &= 2X \\ \dot{x}(t_0) &= nX & \dot{y}(t_0) &= 0\end{aligned}\quad (45)$$

After a quarter a period ($t_f = t_0 + T/4$) the required position is obtained with the relative velocity to the main satellite

$$\dot{x}(t_f) = nX \quad \dot{y}(t_f) = 0 \quad (46)$$

and has to be compensated in order to stop the relative movement. The total fuel consumption is then

$$TFC = 2nX \quad (47)$$

The same end point is also obtained with the same fuel consumption from initial point

$$\begin{aligned}x(t_0) &= 0 & y(t_0) &= -2X \\ \dot{x}(t_0) &= -nX & \dot{y}(t_0) &= 0\end{aligned}\quad (48)$$

and a transition on time of three quarters of a period $t_f = t_0 + 3T/4$.

According to the second manoeuvre the starting point and applied velocity changes are

$$\begin{aligned}x(t_0) &= 0 & y(t_0) &= \frac{3\pi}{4} X \\ \dot{x}(t_0) &= 0 & \dot{y}(t_0) &= \frac{n}{4} X\end{aligned}\quad (49)$$

After one half of the period $t_f = t_0 + T/2$ the required position is reached with the relative velocity to the main satellite.

$$\dot{x}(t_f) = 0 \quad \dot{y}(t_f) = -\frac{7n}{4} X \quad (50)$$

and has to be compensated in order to stop the relative movement. The total fuel consumption using this scenario is again

$$TFC = 2nX \quad (51)$$

The total fuel consumption for both possibilities is the same, the initial point however a bit different (2.00X and 2.36X respectively). With the first possibility the final positions above (positive X) and below (negative X) can be reached from the initial point, which is before or behind the target, with the second scenario however, the final position above (positive X), can be reached only from the initial position before the target, while the final position below the target can be reached from the

initial position behind it. As described earlier in Eq. (15), the follower starts to drift from this constellation. This drift is not negligible; in a typical observation time of 100s, satellite period 6000s and $X=10\text{m}$, the follower would drift for 16.43cm in the Radial and 1.15cm in the In-track direction. This drift can be compensated by a small acceleration $a_x = 3n^2 x(t_0) = 6.58\text{mm/s}^2$. Using impulsive cold gas thruster propulsion with typical $\Delta v = 1\text{mm/s}$ this means a impulse every 7.6s causing a zigzag motion of the follower with the amplitude of 0.95mm in the Radial direction.

Changing the z In-track position.

This manoeuvre changes the z (In-track) position of the follower. From linear equations (6) it is obvious that the Cross-track movement is decoupled from the Radial-In-track motions. However even with the non-linear equations (1) the coupling is negligible. The starting and final points are

$$\begin{bmatrix} x(t_0) \\ y(t_0) \\ z(t_0) \end{bmatrix} = \begin{bmatrix} 0 \\ 0 \\ 0 \end{bmatrix}, \begin{bmatrix} x(t_f) \\ y(t_f) \\ z(t_f) \end{bmatrix} = \begin{bmatrix} 0 \\ 0 \\ Z \end{bmatrix} \quad (52)$$

According to Eq. (14) this can be done in several ways, depending on the time required for transition. Minimal fuel consumption is, if the final time is chosen to be

$$t_{f1} = t_0 + \frac{T}{4} \quad (53)$$

$z(t_f)$ becomes

$$z(t_f) = Z = \frac{\dot{z}(t_0)}{n} \Rightarrow \dot{z}(t_0) = nZ \quad (54)$$

This equation determines the required initial velocity in the Cross-track direction. At the destination position, the follower has zero velocity in the Cross-track direction, so no fuel is needed to stop it. However to keep the follower in this constellation, an acceleration in the Cross-track direction is needed. According to Eq. (14), this is

$$Z = \left[Z - \frac{1}{n^2} a_z \right] + \frac{1}{n^2} a_z \Rightarrow a_z = n^2 Z \quad (55)$$

Circumvolution of the target in the x-y plane

The starting constellation for this manoeuvre is the y (In-track) displacement of the satellites of the magnitude A , which should correspond to the semi-major axis of the circumvolution ellipse. If the satellites

are not in this constellation, a preliminary manoeuvre should be performed first to bring them into the required constellation configuration.

$$\begin{aligned} x(t_0) &= 0 & \dot{x}(t_0) &= 0 \\ y(t_0) &= A & \dot{y}(t_0) &= 0 \\ z(t_0) &= 0 & \dot{z}(t_0) &= 0 \end{aligned} \quad (56)$$

Then a velocity change in the x (Radial) direction is performed. According to Eq. (17) the required velocity change is

$$A = \frac{2}{n} \dot{x}(t_0) \Rightarrow \dot{x}(t_0) = \frac{An}{2} \quad (57)$$

If the follower is behind the target, the velocity change must be performed in the negative x (Radial) direction and if the follower is in front of the target, the velocity change must be performed in the positive x direction. Linear equations (14) now become

$$\begin{aligned} x(t) &= \frac{\dot{x}(t_0)}{n} \sin n(t-t_0) = \frac{A}{2} \sin n(t-t_0) \\ y(t) &= \frac{2\dot{x}(t_0)}{n} \cos n(t-t_0) = A \cos n(t-t_0) \end{aligned} \quad (58)$$

The target satellite is in the centre of the ellipse with the semi-major axis A and the semi-minor axis $A/2$.

Encircling the target

Encircling the target on a circle with radius A can be achieved by the combination of the circumvolution on an ellipse as described in the previous point and an additional linear motion in the z (cross-track) direction. If an additional velocity change in the z direction of magnitude $\dot{x}(t_0)\sqrt{3}$ is applied, the z movement becomes

$$z(t) = \frac{\sqrt{3}\dot{x}(t_0)}{n} \sin n(t-t_0) = \frac{\sqrt{3}}{2} A \sin n(t-t_0) \quad (59)$$

The distance of the follower from the origin (target) is now

$$r(t) = \sqrt{x^2(t) + y^2(t) + z^2(t)} = A \quad (60)$$

The combined movement is thus on a circle with the radius A on a plane which has an inclination of 30° to the y - z plane. If the velocity change in the z direction is performed in the negative direction, the movement is on a circle in the plane with the inclination of -30° to the y - z plane.

ORBIT DEVIATIONS DUE TO ECCENTRICITY

Nonlinear HWC equations are valid for Keplerian orbits without any disturbances, their linearized version (6) for circular (eccentricity $\varepsilon=0$) orbits only. In this section the influence of non-zero eccentricity will be investigated by the method of small deviations (perturbations). First a linear model of equations of the target satellite movement (Eqs. 2, 3) will be obtained for small ε by linearization of orbit deviations from the circular orbit. Next the influence of these deviations on relative position of a satellite will be investigated.

The distance of the leading satellite to the Earth centre point and the time derivative of its true anomaly will be linearized around the semi major axis of the motion ellipse a and around its mean motion n respectively, so they can be expressed as

$$\begin{aligned} R &= a + \Delta R \\ \dot{\varphi} &= n + \Delta \dot{\varphi} \end{aligned} \quad (61)$$

which applied to Eqs. (2) and (3) and using Taylor series yields

$$\begin{aligned} \ddot{\varphi} &= -\frac{2\dot{R}\dot{\varphi}}{R} \Big|_{\substack{R=a, \\ \dot{R}=0, \\ \dot{\varphi}=n}} + \frac{\partial}{\partial \dot{\varphi}} \left(-\frac{2\dot{R}\dot{\varphi}}{R} \right) \Big|_{\substack{R=a, \\ \dot{R}=0, \\ \dot{\varphi}=n}} \Delta \dot{\varphi} + \\ &\frac{\partial}{\partial \dot{R}} \left(-\frac{2\dot{R}\dot{\varphi}}{R} \right) \Big|_{\substack{R=a, \\ \dot{R}=0, \\ \dot{\varphi}=n}} \Delta \dot{R} + \frac{\partial}{\partial R} \left(-\frac{2\dot{R}\dot{\varphi}}{R} \right) \Big|_{\substack{R=a, \\ \dot{R}=0, \\ \dot{\varphi}=n}} \Delta R = \\ &= -\frac{2n}{a} \Delta \dot{R} \end{aligned} \quad (62)$$

and

$$\begin{aligned} \ddot{R} &= (R\dot{\varphi}^2 - \frac{\mu}{R^2}) \Big|_{\substack{R=a, \\ \dot{\varphi}=n}} + \frac{\partial}{\partial \dot{\varphi}} (R\dot{\varphi}^2 - \frac{\mu}{R^2}) \Big|_{\substack{R=a, \\ \dot{\varphi}=n}} \Delta \dot{\varphi} + \\ &+ \frac{\partial}{\partial R} (R\dot{\varphi}^2 - \frac{\mu}{R^2}) \Big|_{\substack{R=a, \\ \dot{\varphi}=n}} \Delta R = \\ &= an^2 - \frac{\mu}{a^2} + 2an\Delta \dot{\varphi} + (n^2 + \frac{2\mu}{a^3})\Delta R \end{aligned} \quad (63)$$

respectively. Applying the well-known equation for the mean motion

$$n^2 = \frac{\mu}{a^3} \quad (64)$$

Eqs. (62) and (63) become

$$\ddot{\varphi} = \Delta \ddot{\varphi} = -\frac{2n}{a} \Delta \dot{R} \quad (65)$$

$$\ddot{R} = \Delta \ddot{R} = 2na\Delta \dot{\varphi} + 3n^2\Delta R \quad (66)$$

and represent a linear model for the deviations ΔR and $\Delta \dot{\varphi}$. Next initial conditions for $\Delta R, \Delta \dot{R}$ and $\Delta \dot{\varphi}$ will be developed. It is supposed that the time starts ($t=0$) when the leader (target) satellite passes the perigee and so its true anomaly $\varphi(0)$ is zero and its distance to the Earth mass point is

$$R(0) = a - f = a(1 - \varepsilon) \quad (67)$$

where f is distance from the centre of the ellipse to the focus. From this equation follows

$$\Delta R(0) = -a\varepsilon \quad (68)$$

At the perigee R has its minimum, so

$$\dot{R} = \Delta \dot{R} = 0 \quad (69)$$

Using well known equations for the true (φ) mean (M) and eccentric (E) anomaly

$$M = n \cdot t = E - \varepsilon \sin E \quad (70)$$

$$d\varphi = \frac{\sqrt{1 - \varepsilon^2}}{1 - \varepsilon \cos E} dE \quad (71)$$

we get for $t=0$ that $\varphi(0) = E(0) = 0$ and

$$\frac{dM}{dt} = n = (1 - \varepsilon \cos E) \frac{dE}{dt} = (1 - \varepsilon) \frac{dE}{dt} \quad (72)$$

and consequently

$$\frac{d\varphi(0)}{dt} = \dot{\varphi}(0) = \frac{\sqrt{1 - \varepsilon^2}}{(1 - \varepsilon)^2} n \quad (73)$$

Using (61) and expanding (73) into Taylor series we get

$$\Delta \dot{\varphi}(0) = \dot{\varphi}(0) - n = \left(\frac{\sqrt{1 - \varepsilon^2}}{(1 - \varepsilon)^2} - 1 \right) n = 2n\varepsilon + \frac{5}{2}n\varepsilon^2 + \dots \quad (74)$$

Equations (65) and (66) have an analytical solution, which will be derived next using the derived initial conditions. The integration of Eq. (65) yields

$$\begin{aligned}\Delta\dot{\phi} &= -\frac{2n}{a}(\Delta R - \Delta R(0)) + \Delta\dot{\phi}(0) = \\ &= -\frac{2n}{a}(\Delta R + \varepsilon a) + 2n\varepsilon = -\frac{2n}{a}\Delta R\end{aligned}\quad (75)$$

Eq. (66) now becomes

$$\Delta\ddot{R} = 2na\left(-\frac{2n}{a}\Delta R\right) + 3n^2\Delta R = -n^2\Delta R \quad (76)$$

and its solution with respect to initial conditions (68) and (69) is

$$\Delta R(t) = -\varepsilon a \cos nt \quad (77)$$

The deviation of the time derivative of the true anomaly from the mean motion now becomes

$$\Delta\dot{\phi}(t) = -\frac{2n}{a}(-\varepsilon a \cos nt) = 2n\varepsilon \cos nt \quad (78)$$

Equations (77) and (78) represent the analytical solution of the linear deviation model (65), (66) with respect to derived initial conditions. Due to changing radius of the orbit and changing radial velocity, also the linear velocity of the main satellite is changed and will be elaborated next.

The orbital velocity of the main satellite is

$$\begin{aligned}v(t) &= R(t)\dot{\phi}(t) = a(1 - \varepsilon \cos nt) \cdot n(1 + 2\varepsilon \cos nt) \approx \\ &\approx an(1 + \varepsilon \cos nt)\end{aligned}\quad (79)$$

where the term with ε^2 was neglected. Introducing

$$v(t) = v_0(t) + \Delta v(t) \quad (80)$$

The nominal velocity v_0 and the deviation of the velocity are

$$v_0(t) = an = \sqrt{\frac{\mu}{a}} \quad (81)$$

$$\Delta v(t) = an\varepsilon \cos nt$$

Next the influence of all above given deviations on the deviations of relative distance of satellites will be investigated.

THE INFLUENCE OF ECCENTRICITY ON THE RADIAL AND IN-TRACK DISTANCES

The deviations of the Radial and In-track distances between satellites from the distance at circular orbit (denoted Δx and Δy respectively) due to non-zero

eccentricity is caused by the In-track distance y and by the radial distance x .

Due to the In-track distance y , the satellites are flying along the same track however they pass the same point (e.g. perigee) with a time shift of Δt

$$\Delta t(t) = \frac{y(t)}{R(t)\dot{\phi}(t)} \approx \frac{y(t)}{a \cdot n} \quad (82)$$

The orbit eccentricity causes that the distance of both satellites from the Earth point mass is not the same all the time; it changes due to the time shift according to

$$\Delta x(t) = \frac{\partial R(t)}{\partial t} \cdot \Delta t = a\varepsilon n \sin nt \cdot \frac{y}{an} = \varepsilon y \sin(nt) \quad (83)$$

Besides also due to different velocities of the satellites the distance between the satellites changes as follows

$$\Delta y_y(t) = \Delta v \Delta t = an \cos nt \cdot \frac{y(t)}{an} = y(t)\varepsilon \cos nt \quad (84)$$

As shown in previous section, at different manoeuvres the follower goes to a higher (slower), or lower (faster) orbit. The velocity on a circular orbit is defined in Eq. (81), so the change in of the velocity due to different orbit (radius) is

$$\frac{\partial v_0}{\partial a} = \frac{\partial}{\partial a} \left(\sqrt{\frac{\mu}{a}} \right) = -\frac{1}{2} \sqrt{\frac{\mu}{a^3}} = -\frac{1}{2} n \quad (85)$$

As system is linearized, this implies

$$\frac{\partial \Delta v}{\partial a} = -\frac{1}{2} \Delta\dot{\phi} = -n\varepsilon \cos nt \quad (86)$$

The influence of the semi-major axis on the deviation of the distances between satellites is

$$\frac{\partial \Delta y_x}{\partial a} = \int_0^t \frac{\partial \Delta v}{\partial a} dt = -\varepsilon \sin nt \quad (87)$$

and the deviation of the distance between the satellites becomes now

$$\Delta y_x(t) = \frac{\partial \Delta y_x}{\partial a} x(t) = -x(t)\varepsilon \sin nt \quad (88)$$

The deviation of the distance becomes now

$$\begin{aligned}\Delta y(t) &= \\ &= -x(t)\varepsilon \sin nt + y(t)\varepsilon \cos nt + C\end{aligned}\quad (89)$$

THE INFLUENCE OF ECCENTRICITY ON CROSS-TRACK DISTANCES

The cross-track deviations due to orbit eccentricity will be derived by the method of perturbations. The relative movement of the main satellite in the LVLH coordinate system of the target is for circular orbit without propulsion and disturbances described by Eq. (6)

$$\ddot{z}_c + n^2 z_c = 0 \quad (90)$$

Where z_c means the z component for circular orbit.

The initial conditions are the velocity changes $\dot{z}(t_0)$ in cross-track direction on the main satellite flying along-track with the target ($z_c(t_0) = 0$).

The analytical solution to this undisturbed flight is

$$z_c(t) \equiv \frac{\dot{z}_c(t_0)}{n} \sin n(t-t_0) \quad (91)$$

By the method of perturbations, the deviation from this solution is described by

$$\Delta z(t) = \varepsilon z_1(t) \quad (92)$$

where ε is a small eccentricity. The z component now becomes

$$z(t) = z_c(t) + \Delta z(t) = z_c(t) + \varepsilon z_1(t) \quad (93)$$

Nonlinear Eq (4) for the z component can be written as

$$\ddot{z} = -\frac{\mu}{R^3} z \approx -\frac{\mu}{a^3} (1 + 3\varepsilon \cos nt) \cdot z \quad (94)$$

and can be using Eq (93) and neglecting terms with ε^2 written as

$$\begin{aligned} \ddot{z}_c + \varepsilon \ddot{z}_1 &= -n^2 (1 + 3\varepsilon \cos nt) (z_c + \varepsilon z_1) \approx \\ &\approx -n^2 z_c - \varepsilon [n^2 z_1 + 3n^2 z_c \cos nt] \end{aligned} \quad (95)$$

According to the method of perturbations the this equation is split into two equations – the original equation for $\varepsilon = 0$ and a new one for z_1 which is obtained by collecting the terms with ε :

$$\ddot{z}_1 + n^2 z_1 = -3n^2 z_c \cos nt. \quad (96)$$

In this equation z_c is solution of the non-disturbed (circular orbit) differential equation (90) with corresponding initial conditions. The initial conditions for the non-homogenous Eq (96) are

$$z_1(t_0) = 0, \quad \dot{z}_1(t_0) = 0 \quad (97)$$

The analytical solution of Eq (96) with initial conditions (97) is

$$\begin{aligned} z_1(t) &= \frac{3}{2n} \dot{z}(t_0) \sin(nt_0) - \frac{1}{n} \dot{z}(t_0) \sin(n(t-t_0)) + \\ &+ \frac{1}{2n} \dot{z}(t_0) \sin n(2t-t_0) \end{aligned} \quad (98)$$

If the manoeuvre starts at perigee ($t_0 = 0$) the deviation Δz becomes

$$\Delta z = \frac{\varepsilon \dot{z}(0)}{n} \left(\frac{1}{2} \sin 2nt - \sin nt \right) \quad (99)$$

If the manoeuvre starts at apogee, ($t_0 = \pi/n$) the derivation Δz changes its sign.

If the manoeuvre starts at mean anomaly $\pi/2$ or $3\pi/2$, the derivation becomes

$$\Delta z = -\frac{\dot{z}(t_0)}{n} (\cos^2 nt + \cos nt - 2) \quad (100)$$

THE INFLUENCE OF ECCENTRICITY ON DIFFERENT MANOEUVRES

In this section the influence of eccentricity on different manoeuvres will be investigated

Along track flying-trailing formations

Applying Eq. (22) to (83) and (89) yields

$$\Delta x(t) = D\varepsilon \sin nt \quad (101)$$

$$\Delta y(t) = D\varepsilon \cos nt \quad (102)$$

The follower is not flying in constant displacement to the main, as it is in a circular orbit. Rather, it is encircling this position on a circle with radius, $D\varepsilon$. The smallest distance between satellites is at apogee, the largest at perigee.

Circumvolution of a point (main) on the track.

Applying Eqs. (16), (17) to (82) and (89) we

$$\begin{aligned} \Delta x(t) &= \left[\frac{2\dot{x}(t_0)}{n} (\cos n(t-t_0) - 1) + y_0 \right] \cdot \varepsilon \sin nt = \\ \text{get} \quad &= \frac{2\dot{x}\varepsilon}{n} \cos n(t-t_0) \sin nt + \left[y_0 - \frac{2\dot{x}(t_0)}{n} \right] \cdot \varepsilon \sin nt \end{aligned} \quad (103)$$

$$\begin{aligned} \Delta y(t) &= - \left[\frac{\dot{x}(t_0)}{n} \sin n(t-t_0) \right] \cdot \varepsilon \sin nt + \\ &+ \left[\frac{2\dot{x}(t_0)}{n} (\cos n(t-t_0) - 1) + y_0 \right] \varepsilon \cos nt \end{aligned} \quad (104)$$

If the manoeuvre starts at perigee ($t_0 = 0$) and the follower is encircling the target ($\dot{x}(t_0) = y(0)n/2$), these equations become

$$\begin{aligned} \Delta x(t) &= \frac{\varepsilon y(0)}{2} \sin 2nt \\ \Delta y(t) &= \frac{\varepsilon y(0)}{4} (3\cos 2nt + 1) \end{aligned} \quad (105)$$

This makes the trajectory of the movement of the follower around main thicker (bigger in the x direction). The influence at the second harmonic is most expressive at the apogee.

If the same manoeuvre starts at apogee, the equations remain the same, but $\Delta y(t)$ changes its sign. The influence of second harmonic is most expressive at perigee.

If the same manoeuvre starts at mean anomaly of $\pi/2$, the equations for deviations become

$$\begin{aligned} \Delta x &= - \frac{\varepsilon y_0}{2} \sin 2nt \\ \Delta y &= \frac{3y_0}{n} \sin 2nt \end{aligned} \quad (106)$$

The trajectory becomes longer (bigger in the y direction). The influence of second harmonic is most expressive at the mean anomaly of $3\pi/2$.

If the same manoeuvre starts at mean anomaly of $3\pi/2$, equations for Δx and Δy remain the same, but Δy changes its sign. The influence of second harmonic is most expressive at the mean anomaly of $\pi/4$.

RESULTS OF SIMULATIONS

Fig.1. represents one of the possible scenarios.

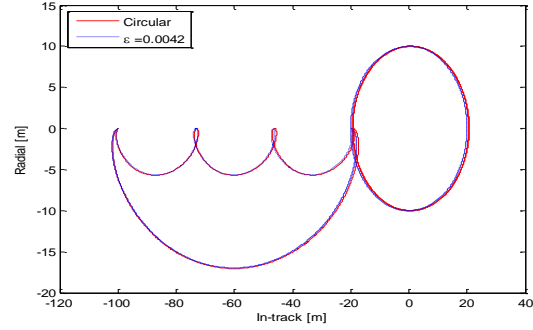


Figure. 1: One of the possible scenarios

The follower starts 100 m behind the target. The linear and nonlinear models for eccentricity 0.0042 were applied. With the nonlinear model all manoeuvres started at apogee. The results for the circular orbit are shown in solid red; the results for the eccentric model in dotted blue. Two nearing approaches to 20 m behind the target were simulated. At the first one, a velocity change of 4.44mm/s in the negative In-track direction was applied and the follower achieved the desired position after one period; at the second one a three times smaller velocity change (-1.48mm/s) brought the follower into the same position after three periods. At this point the follower was stopped in the In-track direction and a velocity change of 10.47mm/s was applied in the negative Radial direction. This caused a circumvolution of the follower around the target on an ellipse with a semi-major axis of 20m and a semi-minor axis of 10m. A detail (transition from nearing approach

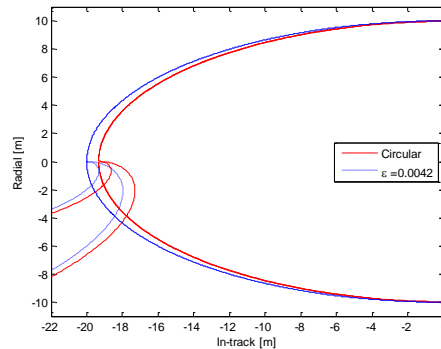


Figure. 2: A detail of Fig.1.

to circumvolution) of this scenario is shown in Fig.2. in the same (In-track – Radial) projection as Fig.1.

It can be seen that the deviation of the position of the follower from the position determined by linear (circular orbit) model due to eccentricity of 0.0042 is 0.67m. After one revolution of the follower around the target, a velocity change of 18.15mm/s was performed into the negative Cross-track direction. The resulting motion is the encircling of the target on a circle with the radius of 20m on an orbit with the relative inclination of 30^0 to the Cross-track - In-track plane. After one encircling a double velocity change of 36.3mm/s was performed to the positive Cross-track direction. This manoeuvre resulted in an encircling of the target on an orbit which was inclined symmetrically with respect to the first encircling. Fig.3. represents the Cross-track – Radial projection of the whole scenario.

In Figs. (4) (5) and (6) respectively, the In-track, Radial and Cross-track deviations due to orbit eccentricity are given. Red curve represents simulated

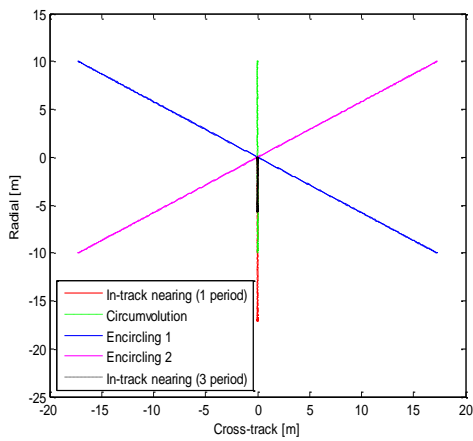


Figure. 3: Cross-track – Radial projection

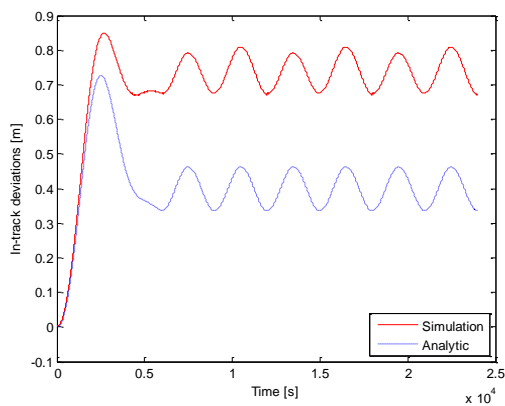


Figure. 4: In-track deviations due to eccentricity

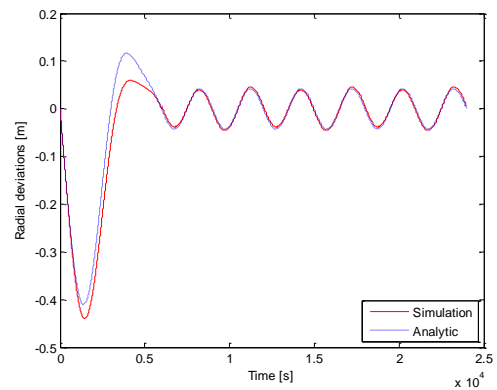


Figure. 5: Radial deviations due to eccentricity

data (nonlinear model) while blue dotted line represents the results of the theoretical model given previously in this paper.

This approach, which is the original contribution of this paper, has proven its applicability, since it can predict the correction of velocity changes due to the true ano-

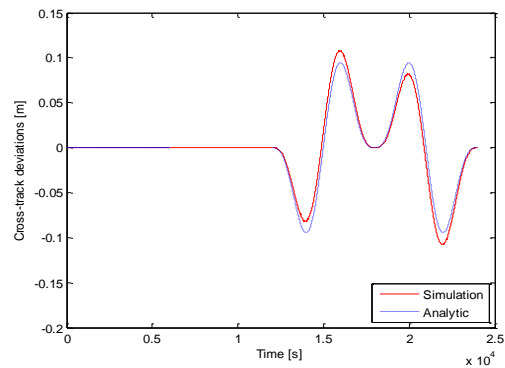


Figure. 6: Cross-track deviations due to eccentricity

maly of the satellite on an eccentric orbit. The predictions for all manoeuvres, except for the repositioning of the satellite on the In-track, are very good. The repositioning the satellite on the In-track needs improvement and optimization, which will be performed in the future.

Fig. (7) represents the In-track, Radial and Cross-track deviations due to the J2 disturbance. It can be seen that the influence of the J2 is in the millimetre range and is far less than the influence of the eccentricity, even if this is very small.

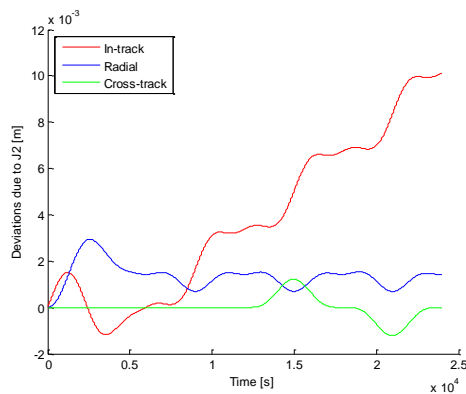


Figure 7: Deviations due to J2 disturbances

Conclusion

Various scenarios suitable for formation flying applications, such as radar interferometric constellation, high-resolution optical dual satellite imaging-fractionated spacecraft and space debris observation were studied with respect to suitable manoeuvres. Required manoeuvres are: parallel flying – in-track, radial and cross-track displacement, circumvolution of the target in the radial – in-track plane and encircling the target on a circle

The scenarios were investigated by mathematical models. First a linear model based on HCW equations was applied with respect to required fuel consumption. Then a linearization of the deviations due to orbit eccentricity was performed by the method of perturbations. This is the main contribution of this paper. The validity of derived models was tested by the simulation of a nonlinear model. It was also established that the influence of the J2 perturbation is much smaller than the influence of eccentricity. It was established that the derived models are quite satisfactory for all manoeuvres but the in-track repositioning of the satellite, which will be performed and optimized in the future.

Acknowledgments

The Centre of Excellence for Space Sciences and Technologies SPACE-SI is an operation partly financed by the European Union, European Regional Development Fund and Republic of Slovenia, Ministry of Higher Education, Science and Technology.

References

1. David A. Vallado, *Fundamentals of Astrodynamics and Applications* (2nd Edition).
2. H. Schaub and J. L. Jinkins, *Analytical Mechanics of Space Systems*, AIAA Educational Series,

AIAA, Reston, VA, 2003, pp. 11-15, 593-673.

3. Pasi Riihimäki, Jean-Peter Ylén, *Simulation of Spacecraft Attitude and Orbit Dynamics*, in: *Proceedings 19th European Conference on Modelling and Simulation, ECMS, Riga, Latvia, 2005*.
4. F. Casella, M. Lovera, *High accuracy simulation of orbit dynamics: an object-oriented approach*, in: *Proceedings of the Sixth EUROSIM Congress, Ljubljana, Slovenia, September 9–13, 2007*.
5. S.R.Ploen, D.P. Scharf, F.Y. Hadaegh and A.B. Acikmese, *Dynamics of Earth Orbiting Formations*, <http://trs-new.jpl.nasa.gov/dspace/bitstream/2014/38974/1/04-1594.pdf>
6. D. R. Izzo, *Formation Flying Linear Modelling*, in: *Dynamics of Systems and Structures in Space, 5th conference, Kings College, Cambridge, July 2002*.
7. Hsi-Han Yeh, A. Sparks, *Geometry and Control of Satellite Formations*, in: *Proceedings of the American Control Conference Chicago, Illinois, June 2000*.
8. V. V. S. S. Vaddi, *Modelling and Control of Satellite Formations*: <http://txspace.tamu.edu/bitstream/handle/1969.1/329/etd-tamu-2003A-2003032711-Veer-1.pdf?sequence=1>
9. R. W. Beard, J. Lawton, F. Y. Hadaegh, *A Coordination Architecture for Spacecraft Formation Control*, *IEEE Transactions on Control Systems Technology*, Vol. 9, No. 6, November 2001, pp. 777–790.
10. P. Sengupta, *Satellite Relative Motion Propagation And Control In The Presence Of J2 Perturbations*, partial fulfillment of the requirements for the degree of MSc, Texas A & M University, 2003.
11. J. S. Ginn, *Spacecraft formation flight: analysis of the perturbed J₂-Modified Hill-Clohessy-Wiltshire equations*, The University of Texas at Arlington, August 2006.
12. L. Yunfeng, M. Xin, G. Yunfeng and L. Xiang,

- Study on relative orbital configuration in satellite formation flying, *Acta Mech Sinica*, vol. 21, pp. 87-94, 2005.
13. S. Nolet, Development of a Guidance, Navigation and Control Architecture and Validation Process Enabling Autonomous Docking to a Tumbling Satellite, partial fulfillment of the requirements for the degree of PhD, MIT, 2007.
 14. H. Schaub, K. T. Alfriend, Impulsive feedback control to establish specific mean orbit elements of spacecraft formations, *Journal of Guidance, Control, and Dynamics*, Vol. 24, No. 4, 2001, pp. 739–745
 15. Dong-Woo Gim and K. T. Alfriend, The State Transition Matrix Of Relative Motion For The Perturbed Non-Circular Reference Orbit, in: *AAS/AIAA Space Flight Mechanics Meeting*, 11-15 February 2001.
 16. M.M. Jeffrey, Closed-loop Control of Spacecraft Formations with Applications on SPHERES, partial fulfillment of the requirements for the degree of MSc, MIT, 2008.
 17. A. Fejzić, S. Nolet, L. Breger, J.P. How, D.W. Miller, Results of SPHERES Microgravity Autonomous Docking Experiments in the Presence of Anomalies, *59th International Astronautical Congress*, Glasgow, Scotland. Sep 29 -Oct 3, 2008.
 18. Pongvthithum, R. , Veres, S. M. , Gabriel, S. B. and Rogers, E., Universal adaptive control of satellite formation flying, *International Journal of Control*, vol. 78, no. 1, 2005, pp. 45–52
 19. M.S. de Queiroz, Q. Yan, G. Yang, V. Kapila, Global Output Feedback Tracking Control of Spacecraft Formation Flying with Parametric Uncertainty, in: *Proceedings of the 38th Conference on Decision & Control*, Phoenix, Arizona USA, December 1999.
 20. Q. Wu, M. Saif, Robust Fault Detection and Diagnosis for a Multiple Satellite Formation Flying System Using Second Order Sliding Mode and Wavelet Networks, in: *Proceedings of the 2007 American Control Conference*, New York City, USA, July 11-13, 2007.
 21. N. C. Nuzzo, Effects of Propagation Techniques on Relative GPS Navigation, partial fulfillment of the requirements for the degree of MsC, US Naval Academy, 1997.
 22. A. Fejzić, Development of Control and Autonomy Algorithms for Docking to Complex Tumbling Satellites, partial fulfillment of the requirements for the degree of MsC, MIT, 2008.
 23. K. T. Alfriend and H. Schaub, Dynamics and Control of Spacecraft Formations: Challenges and Some Solutions, *Journal of the Astronautical Sciences*, Vol. 48, No. 2, 2000, pp. 249–267.
 24. S. R. Vadali, S. S. Vaddi, K. T. Alfriend, An intelligent control concept for formation flying satellites, *International Journal of Robust and Nonlinear Control*, Vol. 12, 2002, pp. 97–115
 25. Relative Navigation for Formation Flying of Spacecraft R. Alonso, Ju-Young Du, D. Hughes, J. L. Junkins, J. L. Crassidis, in: *2001 Flight Mechanics Symposium*, 01 June 2001. pp. 115–129
 26. R. Alonso, J. Crassidis and J.L. Junkins, Vision-based relative navigation for formation flying of spacecraft, in: *Proceedings of the 2000 AIAA, GNC Conference*, Denver, CO, August 2000, Paper 2000-4439.
 27. Breger, L., J. P. How, GVE-Based Dynamics and Control for Formation Flying Spacecraft, http://acl.mit.edu/papers/BregerHow_Paper.pdf
 28. Richards, J.A., *Remote sensing with Radar*, Signal and Communication Technology, Springer 2009.
 29. Yang Z., Yang R., Feasibility Study of Using Small Satellite Synthetic Aperture Radar for Global 3D Imaging, 0-7803-7536-X 2002 IEEE
 30. Kun R., V. Prinet, X. Shi, F. Wang ,Comparison Of Satellite Baseline Estimation Methods For Interferometry Applications, 0-7803-7929-2/03/ 2003 IEEE.